J. Webster (ed.), *Wiley Encyclopedia of Electrical and Electronics Engineering*

PYROMETERS

Infrared (*IR*) temperature measurement has been in use for a century. It has gained wide acceptance in industry and science wherever the target of interest cannot be contacted because it is too hot, moving or, for other reasons, not accessible to a contact probe such a resistance or thermocouple element. The worldwide annual market for IR pyrometers is now around $\frac{1}{4}$ billion US dollars. There are about two dozen firms offering pyrometers, the most important of which are listed in Table 1.

The following sections deal with concepts and implementation of all practical pyrometers that are in use today or are about to enter the market.

Fundamentals of Pyrometry

At temperatures above absolute zero all bodies emit electromagnetic radiation. Planck's radiation law (1) describes the relationship between a body's surface temperature and the associated spectral radiance

$$L(w, T) = E(w, T)c_1 w^{-5}[\exp(c_2/wT) - 1]^{-1} \qquad (1)$$

where $L(w, T)$ is the spectral radiance as a function of wavelength W and absolute temperature T. $C_1 = 3.7413 \times 10^{-12}$ W $\cdot$ cm^2, $C_2 = 1.4388$ cm $\cdot$ degree are the first and second radiance constants, and $E(w, T)$ is the spectral emissivity of the surface, which also is a function of temperature. For a black body $E(w, T) = 1$. Figure 1 shows graphs of spectral radiance vs. wavelengths for different temperatures T, the so-called Planck curves. For all other bodies $E(w, T) < 1$. From Eq. (1) then follows that $E(w, T)$ is the ratio of the radiance of a surface at a certain temperature T to the black body radiance at the same temperature T. A special case occurs when $E(w, T) =$ constant < 1. Such objects are called gray bodies. The Planck curves exhibit several important features (see Fig. 1):

(1) They do not intersect each other, which means that the radiance at any wavelength increases monotonically with temperature.
(2) For each temperature there is a wavelength of peak emission that shifts to longer wavelengths with decreasing temperature. This shift is expressed by Wien's displacement law (2)

$$w_{\max} \cdot T = 2897.6\ \mu\text{m} \cdot \text{degree}$$

(3) If one sets $E(w, T) = 1$ and integrates Eq. (1) over all wavelength, one gets the Stefan–Boltzmann law for the total radiance of a black body:

$$L_{\text{tot}} = s^* T^4$$

Table 1. List of Pyrometer Companies

Cino Co., Ltd., 32-8, Komano-cho, Itabashi-ku, Tokyo 173
Phone 011 3 3956 211; fax 011 3 3956 0915

Impac Electronic Gmbh, Krifterler Strasse 32, D-60326 Frankfurt/M, Germany
Phone 011-49-69-9 73 73-0; fax 011-49 69-9 73 73-181

IRCON, Square D Company, 7301 N. Caldwell Ave., Niles, IL 60648
Phone 708-967-5151; fax 708-647-0948

Keller GmbH, In der Garte 40, D-49479 Ibbenbüren, Germany
Phone 011-49-5451-85-0; fax 011-49-5451-412

Land Instruments International, Ltd., Dronsfield, S18 1DJ, UK
Phone +44 (1266) 417 691; fax +44 (1266) 290 274

Luxtron, 2775 Northwestern Pkwy, Santa Clara, CA 95051-0951
Phone 1-800-627-1666 or 1-408-727-1600; fax 1-408-727-1677

Mauer (Dr. Georg) GmbH, Industriegebiet 10, D-72664 Kohlberg, Germany
Phone 011-49-7025-3031; fax 011-49-7025-6053

Mikron Infrared Co. Ltd., 16 Thornton Road, Oakland, NJ 07436
Phone 1-201-405-0900; fax 1-201-405-0090

Minolta Camera Co., Ltd., 30, 2-Chome, Azuchi-Machi, Higashi-Ku, Osaka 541, Japan

Pyrometer Instruments Co., Inc., 234 Industrial Pkwy., P.O. Box 70, Northvale, NJ 07647
Phone 201-768-2000; fax 201-768-2570

Quantum Logic Corp., Box 191, Westport CT 06881
Phone 203-226-3541; fax 203-227-8240

Raytek, Inc., 1201 Shaffer Rd., Box 1820, Santa Cruz, CA 95061-1820
Phone 408-458-1110; fax 408-458-1239

Tokio Seiko, 1-1 Kozura-Cho, Chigasaki-City, Kanagawa-Pref. 253, Japan
Phone 011/ 81 467 546522; fax 011/ 81 467 546177

Williamson, 70 Domino Dr., Concord, MA 01742
Phone 1-617-369-9607

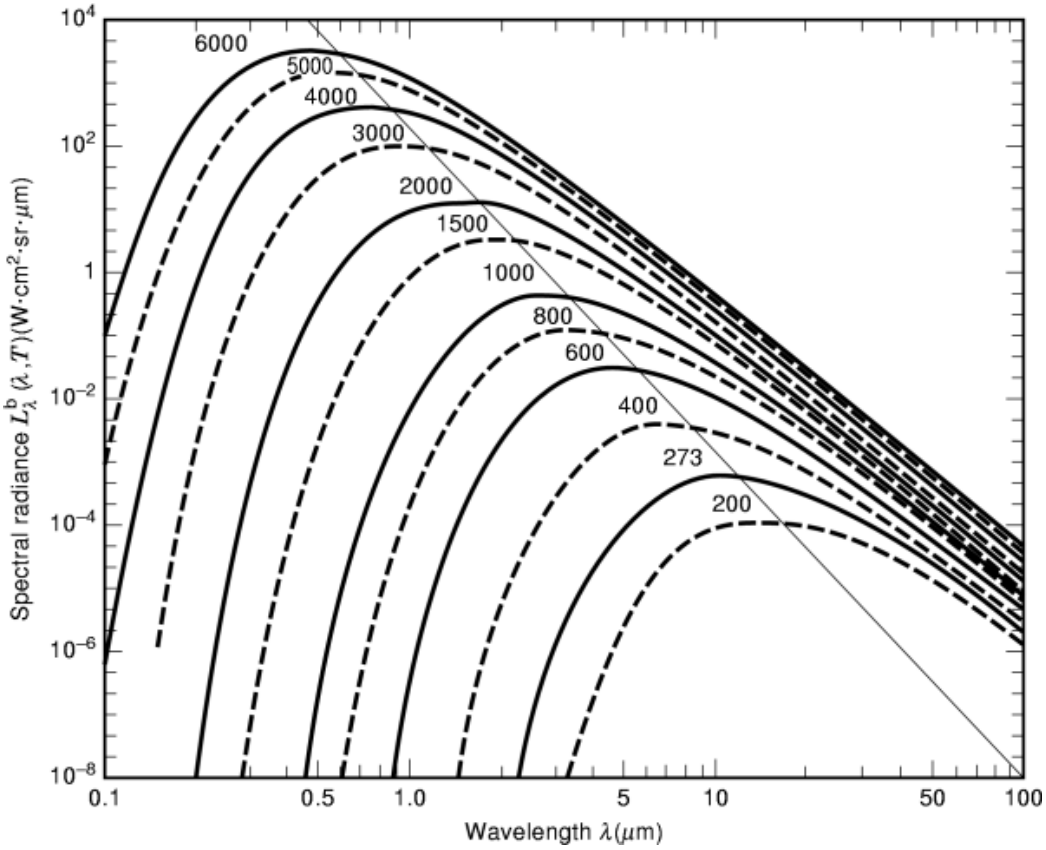

Fig. 1. Planck curves (curves are for constant blackbody temperature, in K).

where $s = 5.669 \times 10^{-12}$ W · cm^2 · degree^{-4} is the Stefan–Boltzmann constant. If the object is *not* a black body, the total radiance is given by

$$L_{\text{tot}} = E^*_{\text{eff}} s^* T^4$$

where E_{eff} is an effective emissivity.

Total Radiance Systems. The emissivity functions $E(w, T)$ depend on the chemical composition of the surface and its texture. Emissivity values have been measured and tabulated for many different materials, but even a thin coating by a different material can change the emissivity drastically. One important industrial example is hot steel being sheared in a processing plant, exposing a pure iron surface. The emissivity of pure steel is about 0.40 in the near infrared spectrum. Hot steel oxidizes rapidly, thereby increasing the emissivity, which can double the emissivity in minutes. Another example is from the semiconductor industry, namely that of a silicon wafer during thermal processing. Such a wafer would typically have on its surface films of materials with different optical refraction indices than that of the silicon substrate. The emissivity of such a wafer is substantially changed from that of the uncoated wafer due to optical interference effects, which occur on such coated surfaces, and which depend strongly on the wavelength of observation. Great temperature errors can result in both above cases if the change in emissivity is not taken into account.

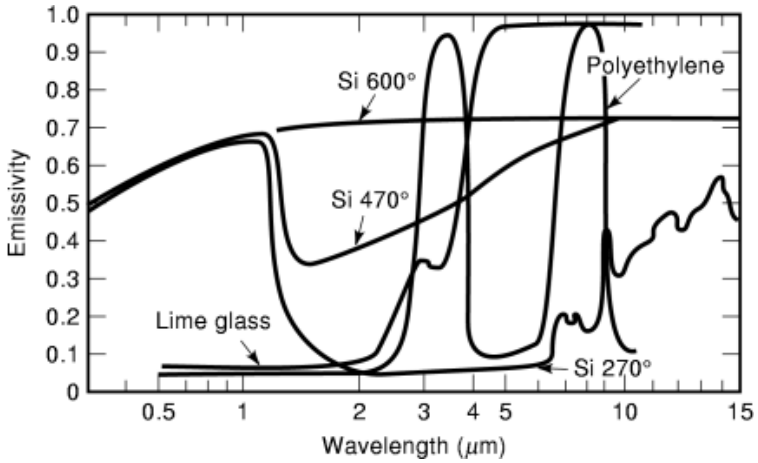

Fig. 2. Spectral emissivity of materials: silicon at 270, 470, and 600°C; lime glass at 500°C; polyethylene at 50°C.

The oldest automatic instruments measured the radiance over the whole infrared spectrum. This yields the most radiative power at the detector, which in early days was a thermocouple element of very low responsivity requiring a maximum of radiant power.

Narrow-Bond Systems. With the development of more sensitive detection methods, particularly quantum detectors coupled to transistor amplifiers, it became feasible to measure small spectral portions of the radiant spectrum. There are several reasons why one wants to use small portions of the radiant spectrum:

(1) The shorter the wavelength, the steeper the local exponential slope of radiance versus temperature. Operating at the shortest possible narrow-wavelength band minimizes temperature error due to emissivity uncertainty and calibration drift.
(2) Some materials are opaque at certain wavelength bands. Spectral absorption curves for several materials are shown in Fig. 2.
(3) Multiwavelength pyrometry.

Wavelength Choices. As illustrated by the Planck curves, the radiance peaks shift to longer wavelengths as the target temperature decreases. It is therefore necessary to match the operating wavelength band of the pyrometer to the temperature range of interest. Here one must consider the available radiation detectors (3). The major detectors and their associated temperature ranges are listed in Table 2. For free radiating targets, one should work at the shortest wavelength at which one still obtains reasonable signals. At this point the local exponential slope and the suppression of temperature errors are largest.

Disappearing-Filament System. Prior to the widespread use of infrared detectors, optical pyrometers were the instruments of choice. The operating principle is a visual comparison of the brightness of an electrically heated wire to that of the target seen through a red filter within the pyrometer's viewing optics. By varying the electrical current in the wire, one can adjust its brightness until it blends into the target surface. The wire current is then a measure of the target's radiance temperature. The drawback with these instruments is that they require operator judgment, which may differ from person to person. Also there is usually no provision for emissivity correction.

A newer version of this instrument projects a bright line of variable intensity into the field of view. The line illumination is provided by a small commercial lamp. Its intensity is monitored by a silicon photodetector.

Table 2. Lower Temperature Limits

Lower Limit of Temperature	Infrared Detector[a]	Wavelength (μm)
600°C	Si	0.4–1.0
200°C	Ge and InGaAs	0.8–1.8
100°C	PbS	1.0–3.6
50°C	PbSe	1.5–5.8
−50°C	Pyroelectric detector	No wavelength dependency

[a] Operating at room temperature.

Another method is to hold the filament at a constant temperature, and use a narrow filter coupled with a neutral density filter to match the brightness of the filament with the target.

Dual-Wavelength Method. Dual-wavelength pyrometers exploit the nonlinearity of the Plank equation by determining the temperature from the radiance ratio at two different wavelengths (4). Here, uncertain emissivity ratio leads to error. The real advantage of dual-wavelength pyrometers over single-wavelength systems is the insensitivity of the dual-wavelength measurement to partial obstructions in the line of sight such as dust, steam, and vignetting, since both radiance values attenuate by the same factor. For the same reason there is no lower limit to the target size, as long as the signals at the two wavelengths are measurable.

Active Method. In the following we distinguish between passive and active pyrometry. The former are the traditional instruments which only *receive* radiation, hence the term "passive." New types of pyrometer have been introduced in the last decade, which augment the traditional optical receiver with a reflectometer, sending radiation to the target as well receiving radiation from it; thus the term "active." The fundamental shortcoming of passive pyrometry, namely, its dependence on an estimate of emissivity, was recognized from its inception. For pure materials, such as most metals, the emissivity is known from special sample measurements. But even a thin oxide surface layer can change the emissivity drastically, leading to large temperature errors. In 1905, Rubin (5) proposed a method of measuring the target emissivity E by recognizing that for opaque bodies their hemispheric reflectivity R_{hemisph} is always the unity complement to its emissivity, $E = 1 - R_{\text{hemisph}}$. When a distant target reflects diffusely, R_{hemisph} (and therefore E) can be determined from a measurement of the reflected energy into a relatively small solid angle (6). In practice, one calibrates the reflectance measurement against a diffuse surface of known reflectivity, such as $CaCO_3$ at a known distance d_c and then scales all reflectance values of proper targets at distance d by the factor $(d/d_c)^2$. This is so, since for a particular receiver system the solid angle over which reflected radiation is collected scales with the square of the target distance. The reflectance measurement must, of course, be made at the same wavelength as the radiance measurement. This method is also referred to as "reflection-supported pyrometry."

Furnace Applications. Objects are placed into furnaces to heat them up. By the nature of this process, such objects (targets) are surrounded by heat sources of higher radiance temperature than their own. Reflected ambient radiance can be as large or even larger than the target's thermal self-emission. An interesting situation occurs when the ambient irradiance is isotropic and its radiance temperature is equal to the target temperature. In that case the target appears as if it were a black body (Appendix 1). In general, however, the furnace is hotter than the target and one must separate the thermal target radiance from the reflected furnace radiation because only the former is associated with the target temperature. There is a family of active pyrometers that is designed for this application. These pyrometers have provisions to measure the average ambient radiance

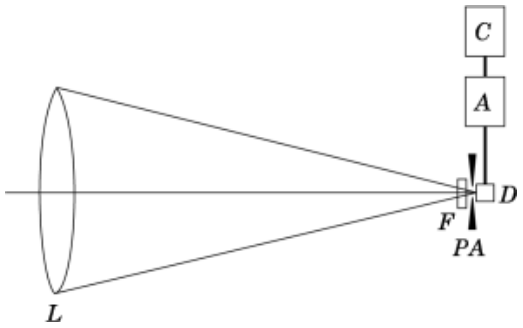

Fig. 3. Passive single-wavelength system. *D*, detector; *F*, filter; *L*, objective lens; *PA*, pinhole aperture; *A*, amplifier; *C*, computer.

as well as the target reflectance. A microcomputer then subtracts the target radiance from the total radiance and then calculates the temperature from the former.

Practical Designs

The following is a description of the pyrometer types that are commercially available at present. Total radiation and optical pyrometers are either being phased out or used for special applications only. Narrow-wavelength and dual-wavelength systems dominate the market. Active pyrometers, a newer type of instrument, are gaining acceptance where accurate temperature measurements are required.

Narrow-Wavelength Pyrometers. The simplest pyrometer design, illustrated in Fig. 3, employs a lens (*L*), a pinhole aperture (*PA*), an optical filter (*F*), and a detector (*D*), with an output signal that is amplified by circuit (*A*) and then applied to microcomputer (*C*), which calculates the temperature from *L* and a manual input for the emissivity *E* via the Planck equation (1).

The temperature is then displayed in digital form (*DS*). One counterintuitive, but, nevertheless, valid feature of that design is that the radiance signal yielded by the detector is independent of the target distance. In other words, if the target moves out of focus, the detector signal remains the same. This very important feature is proven in Appendix 2. More advanced instruments are of the focusing type in which the lens (*L*) is adjustable to image the target surface onto the detector plane. An additional refinement is to reimage the pinhole onto the detector with an auxiliary optical system (7). This latter design reduces stray radiation on the detector and thereby yields the highest degree of angular selectivity.

The dependence of temperature error on emissivity uncertainty can be analyzed by differentiating Eq. (1) with respect to *E*:

$$dT/T = (wT/c_2)dE/E \qquad (2)$$

Equation (2) shows that for any given uncertainty in radiance or emissivity, the corresponding temperature error is smaller by the factor wT/c_2; that is, the shorter the wavelength, the smaller the temperature error, with all thing being equal. Of course, at shorter wavelengths the signal falls off exponentially. This puts a lower limit on the choice of wavelength for any given temperature. There are about a dozen companies that offer a complete assortment of narrowband pyrometers to cover the range of industrially important applications.

Dual-Wavelength Pyrometers. Figure 4 illustrates the design of one version of a dual-color system. A dichroic beam splitter M is placed in the optical path to separate the two wavelength components. One uses two

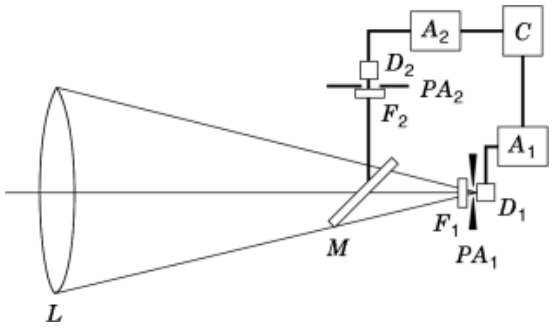

Fig. 4. Passive dual-wavelength system. D_1, detector for wavelength 1; D_2, detector for wavelength 2; F_1, filter for wavelength 1; F_2, filter for wavelength 2; M, dichroic mirror; PA_1, pinhole aperture for wavelength 1; PA_2, amplifier for wavelength 2.

filter-detector-amplifier systems F1-D1-A1 and F2-D2-A2 to measure the respective radiances. Both signals are applied to the microcomputer (C), which calculates the target temperature from the formula

$$T = [(c_2/T)(1/w_2 - 1/w_1)]/[\ln(L_1/L_2)(E_2/E_1)(w_2/w_1)^5] \quad (3)$$

with a manual input for emissivity ratio E_1/E_2. The dual-wavelength systems on the market employ wavelength combinations in the near- and mid-infrared regions: 0.7/0.9, 0.9/1.55, and 3.2/3.7 μm (8).

Active Pyrometers. By adding a reflectometer function, an ordinary pyrometer is transformed into an active instrument illustrated in Fig. 5, where the beam of a pulsed light source (LA), such as a laser, is superimposed onto the pyrometer's optical axis by a beam combiner (M_2). To normalize the outgoing radiation pulse, a beam splitter (M_1) diverts a small portion of the outgoing radiation onto a second, reference detector (D_1), whose output, after amplification, V_2, is applied to a microcomputer (C). The radiance received by detector D consists of a dc component V_0 associated with the thermal target radiance and a superimposed pulsed component of height V_1, which is associated with the reflected pulsed radiation. Timing signals (TR), synchronously generated with the outgoing pulsed radiation, are used by the amplifiers (A) and (A_r) to separate the pulses from the dc component. Finally, a signal V_3 associated with the target distance d is also applied to the computer. When the lens (L) is carefully focused onto the target, the position of this lens relative to its infinity focus location is a measure of the target distance from the lens. Thus, by indexing this relative lens position, monitored by the distance encoder EN, one generates signal V_3 to determine the value of d. This is then used in the following formula to calculate the in situ target emissivity:

$$E = 1 - c_{23}(V_1/V_2)/d^2 \quad (4)$$

The radiance component is proportional to V_0,

$$L = c_{20}V_0 \quad (5)$$

where c_{23} and c_{20} are instrument constants. After determining d from V_3, the computer calculates the temperature T from V_0, V_1, and V_2 via Eqs. (4), (5), and (1).

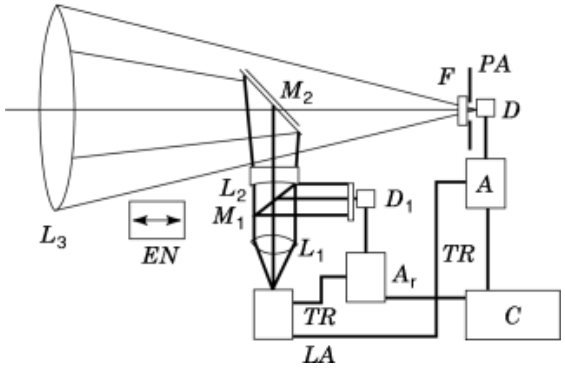

Fig. 5. Active single-wavelength system. D, detector; D_r, reference detector for laser output; F, filter; A, signal amplifier; A_r, reference signal amplifier; L_1, laser collimating lens; M_1, beam splitter for the laser beam; L_2, diverging lens; L_3, objective lens; M_2, mirror; PA, pinhole aperture; C, computer; EN, distance encoder.

Fiber-Optic Systems

All pyrometers of the preceding type can in principle be designed as fiber-optic models. The main advantage of fiber systems is their optical flexibility. While large-lens-type pyrometers require a straight, large-aperture line of sight, fiber systems make pyrometer measurements possible for very restricted and indirect optical access. Ordinary fiber cables have no imaging property; they simply collect over the acceptance angle of the fiber (about 20° for a typical clad quartz system). Also, normal fiber cables use polyvinyl chloride (*PVC*) jackets and must, therefore, stand off from a hot target. Hence the target spot would grow quickly with distance. One therefore places either a sapphire light pipe or a lens system in front of the fiber cable. A sapphire light pipe is extremely heat resistant and can be placed very close to a hot surface in order to make the target spot small. Another method is to stand off from a hot surface and use a lens to image the desired target spot onto the fiber end face. The other end of the fiber cable is placed close to a photodetection system, which sends its output to a signal-processing system. A schematic drawing of a fiber-optic pyrometer is shown in Fig. 6. Fiber-optic cables have wavelength restrictions. If we take 1 dB/m attenuation as a somewhat arbitrary spectral cutoff criterion, water-free quartz fibers transmit from about 0.5 μm to about 2.5 μm (9). Sapphire fibers transmit from 0.5 μm to 4 μm (10), and chalcogenide (As-Se-Te) fibers transmit from 3.0 μm to 9.5 μm (11). Together, these three fiber types cover the most important spectral ranges of pyrometry. In principle, therefore, all these types of pyrometers can be designed as fiber-optic models.

New Developments

Active Dual-Wavelength Pyrometers. Active pyrometry operating at one wavelength has been making very accurate temperature measurements when the target surfaces are diffuse. But there are many more applications for which the surface scattering is somewhere between specular and diffuse, and for which single-wavelength active pyrometry will therefore not work. For these cases the dual-wavelength active technique was developed (12,13).

If one assumes that the polar scattering of a target surface is wavelength independent, one can prove that a measurement of the radiances at two wavelengths and the *ratio* of retroreflectances yields the target emissivity E_1. Since only the ratio of reflectances is needed, the method works for any polar scattering pattern.

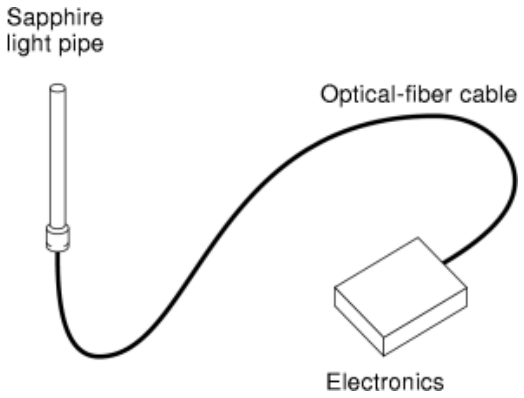

Fig. 6. Typical fiber-optic pyrometer.

The formula for E_1 developed in Ref. 13 has the form

$$E_1 = 1 - R + RB(E_1)^n \tag{6}$$

where

$$B = [L_2(w_2)^5/c_1]/[L_1(w_1)^5/c_1]^n \tag{7}$$

$$n = w_1/w_2 \tag{8}$$

Equation (6) can be solved by successive iteration. From E_1 and L_1 follows the temperature T via the Planck equation (1).

Figure 7shows a system demonstrated in Ref. 13. A bifurcated optical fiber is used to superimpose the illuminating and optical receiver systems. The lamp radiation is mechanically chopped and the reflected energy is synchronously amplified by a lock-in circuit so as to distinguish it from the dc radiance photo signal. The optical receiver uses a di-chroic prism beam splitter to separate the two wavelength components. Additional spectral selection is provided by filters 1 and 2, located in front of detectors D_1, D_2, respectively. Reflection and thermal emission signals for both wavelengths are digitized by an *ADC* and applied to a *PC* for calculation of emissivity and temperature via equations (6), (7), and (1).

Ripple Pyrometry. Ripple pyrometry, another interesting technique is used to measure and control the temperature of silicon wafers heated by quartz-halogen lamps in various rapid thermal processors (14). The ripple method dynamically determines emittances by sensing time-dependent components in radiation from the lamps and radiation reflected by the wafer surfaces; see Fig. 8. A sapphire light probe (S_1) is used to detect radiation from a region on the wafer surface. A second sapphire light probe (S_2) is directed towards the heating lamps and measures the radiation incident on the wafer surface, including secondary reflected radiation. The radiation from sapphire probes S_1 and S_2 is coupled via optical fibers to separate photodetectors. The quartz-halogen lamps are ac powered and therefore exhibit a 120 Hz ripple on top of a dc radiance component, which gives rise to ac photosignals dI_1 and dI_2, as well as dc photosignals I_1 and I_2. According to Ref. 14 the wafer radiance L_w and its reflectivity r_w are related to the ac and dc signals as follows:

$$L_w/(1 - r_w) = (s_1^{-1}I_1 - s_2^{-1}RI_2)/(1 - R) \tag{9}$$

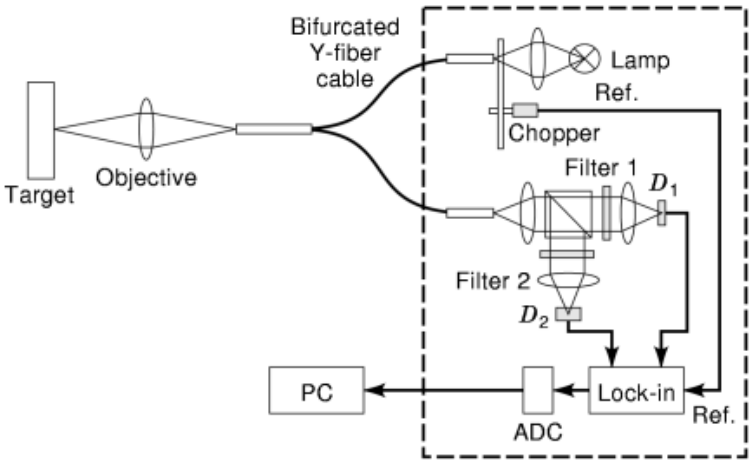

Fig. 7. Two-color active pyrometer. ADC, analog-to-digital converter; D_1, D_2, photodetectors.

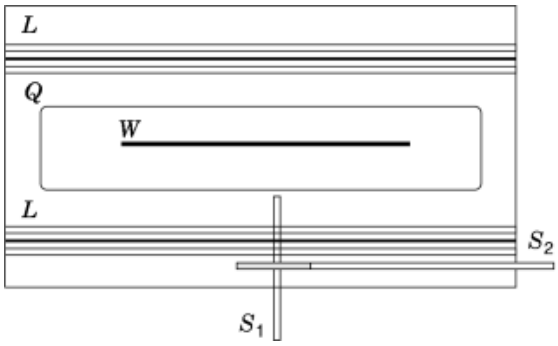

Fig. 8. Schematic cross-sectional view of an RTP furnace showing wafer (W), lamps (L), quartz isolation tube (Q), and optical-fiber probes for the wafer (S_1) and the lamps (S_2). Arrows indicate the directions of the radiances in the model of Eq. (1).

where the effective emittance $1 - R$ and reflectance R are defined in terms of the ratio of the ac components in the two detector signals, according to

$$R = (s_1/s_2)(dI_1/dI_2) \qquad (10)$$

Here s_1 and s_2 are instrument constants. The left-hand side term of Eq. (9) is the blackbody temperature associated with the true wafer temperature and thus yields that temperature. This method has been used to measure wafer temperatures during rapid thermal annealing, an important technique in manufacturing microelectronic devices. Wafer annealing at a temperature of 660°C was monitored with an accuracy of better than 3°C at 1 standard deviation (15).

There are two other types of pyrometer designs which aim to eliminate the emissivity error, multiwavelength pyrometer (16) and the polaradiometer (17), which works best for specular, metallic targets. Multiwavelength systems match the radiance at three or more wavelengths to the Planck formula with some assumption about the spectral emissivity characteristic of the target surface.

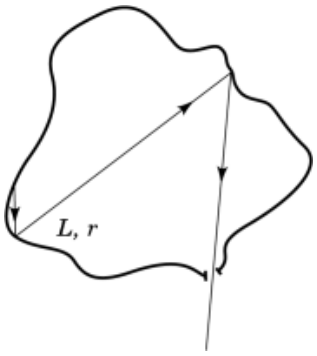

Fig. 9. Hollow blackbody. L, surface radiance; r, surface reflectance. The enclosure at uniform temperature emits like a blackbody independent of the physical emissivity of the inside wall material.

The polaradiometer illuminates a specular target spot from 45° off normal with radiation from a black body while observing, from the mirror image direction, the sum of reflected and thermally emitted radiance with a polarization-analyzing optical receiver. The radiation emitted into an angle far off normal by a hot metal is such that the dominant component of polarization is E_1 (in the plane of incidence) with a lesser component E_2 (perpendicular to the plane of incidence). Since Kirchhoff's law holds for each component, the originally unpolarized black body radiation, when reflected, has R_2 as the dominant component of reflection, the lesser component R_1. One varies the temperature of the black body illuminator, until the combined intensity of emitted and reflected radiation is the same for the two principal polarizations. At that point the temperature of the target is equal to that of the black body.

Both the multiwavelength and the polarization-compensating pyrometers are limited to very special applications, and are not really commercial at this point.

Appendix A. Blackbody Conditions in Furnaces

When making temperature measurements of objects inside furnaces, the influence of reflected radiation must be taken into account in order to determine the correct target temperature. One way to do this is to define an effective emissivity E_{eff}. Consider a hollow enclosure of arbitrary shape with a small opening (Fig. 9).

Assume now that the inside surface is at uniform, elevated temperature. We call L_{bb} the black body radiance of the surface, r the surface reflectivity, and the physical emissivity is E is unity, where once again $E = 1 - r$. Radiation from any point A on the inside surface is the sum of the thermal emission at that point, EL_{bb}, and reflected energy $r(1 - r)L_{\text{bb}}$ emanation from all other points on the internal surface. That radiation itself is of course also the sum of thermal self-emission and reflected radiation from other points on the surface, and so forth at infinitum.

The observed radiance therefore is equal to the infinite sum:

$$L_{\text{obs}} = L_{\text{bb}}(1-r) + L_{\text{bb}}(1-r)r + L_{\text{bb}}(1-r)r^2 + L_{\text{bb}}(1-L)r^3 + \cdots \tag{A.1}$$

This equation can be written in the form

$$L_{obs} = L_{bb}(1-r)(1+r+r^2+r^3+\cdots) \qquad \text{(A.2)}$$

Noting that the sum of the infinite series inside the curly bracket equals $1/(1-r)$, one obtains

$$L_{obs} = L_{bb}(1-r)[1/(1-r)] = L_{bb} \qquad \text{(A.3)}$$

which means the total radiance emanating from the small opening is that of a black body at the temperature of the internal wall, independent of the reflectivity (emissivity) of the wall. Note that this analysis ignores the effect of radiation escaping through the opening. This is permitted if the area of the opening is small compared to the total internal wall area of the hollow space.

Appendix B. Out-OF-Focus Targets

Most on-line pyrometers have a fixed focus. In general one tries to select the optics such that the target is in focus. But in many practical cases, the target ends up somewhat out-of-focus because the installation procedure is not precise. Sometimes the target distance changes such as for objects on a conveyer belt. When the instrument is calibrated by focusing at the opening of a blackbody furnace and is used in the field against a target that is out of focus, the question arises: How does this affect the calibration? Not at all! In the following we will verify by analysis this experimental fact.

If the optics is focused at distance a_1, but the target is located at distance a_3, the power impinging on the detector can be calculated with the help of a ray optics construction illustrated in Fig. 10. A circular detector aperture of diameter d_1, located at image distance b_1 from the lens, corresponds to a circular target area at object distance a_1 of diameter M_1 on the other side of the lens. The object and image distances are related as

$$1/a_1 + 1/b_1 = 1/f \qquad \text{(B.1)}$$

where f is the focal length of the lens. The diameter M_1 is given by

$$M_1 = d_1(a_1/b_1) \qquad \text{(B.2)}$$

The optical power passing through the detector aperture is proportional to the etendue:

$$(M_1)^2(D/a_1)^2 \qquad \text{(B.3)}$$

where the term in the second set of parentheses represents the solid angle subtended by the lens as seen from the object plane. Imagine now that the target is moved to a new location at distance a_3 from the lens. By geometric analysis of the rays running from the edges of the lens to the edges of the target spot at a_1, one can show that the spot diameter at distance a_3 is

$$M_3 = (a_3/a_1)(M_1 - D) + D \qquad \text{(B.4)}$$

where D is the diameter of the lens.

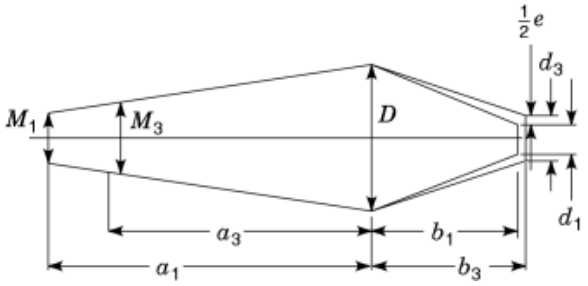

Fig. 10. Spot diameters versus object distance. The edge ray construction is used to calculate the changes in target spot diameter and etendu.

Consider then a radiating disk of diameter M_3 at distance a_3 from the lens. The associated image distance b_3 on the other side of the lens is determined from

$$1/a_3 + 1/b_3 = 1/f \qquad \text{(B.5)}$$

The image diameter

$$d_3 = d_1 + e \qquad \text{(B.6)}$$

is larger than the detector aperture d_1. Thus only a certain fraction of the imaged radiation passes through the aperture. A first-order approximation is to set the fraction of transmitted energy equal to

$$(d_1/d_3)^2 = [d_1/(d_1 + e)]^2 \qquad \text{(B.7)}$$

where

$$e = (D/b_3)(b_3 - b_1) = Db_1(1/b_1 - 1/b_3) \qquad \text{(B.8)}$$

Hence, the power passing through the aperture is proportional to

$$(M_3)^2(D/a_3)^2[d_1/(d_1 + e)]^2 \qquad \text{(B.9)}$$

which is the etendue for an out-of-focus target.

In the following we will prove that the etendues (and hence the photosignals) for in-focus and out-of-focus targets are identical. For this purpose we may consider just the square roots of the respective etendues. Then, we normalize the aperture diameter $d_1 = 1$ in Eq. (B.9) without loss of generality. Next, we substitute e from Eq. (B.8), and M_3 from Eq. (B.4) into Eq. (B.9) and arrive at the expression:

$$D[1/a_3][(a_3/a_1)(M_1 - D) + D]/[1 + Db_1(1/b_1 - 1/b_3)] \qquad \text{(B.10)}$$

The two rectangular brackets in the numerator of Eq. (B.10) can be consolidated and written as

$$M_1/a_1 + D(1/a_3 - 1/a_1) \qquad \text{(B.11)}$$

From Eqs. (B.1) and (B.5) follow

$$1/a_3 - 1/a_1 = 1/b_1 - 1/b_3 \qquad \text{(B.12)}$$

We substituted Eq. (B.12) in (B.11) and (B.10) to arrive at

$$D[M_1/a_1 + D(1/b_1 - 1/b_3)]/[1 + Db_1(1/b_1 - 1/b_3)] \qquad \text{(B.13)}$$

In Eq. (B.13) we substitute $b_1 = a_1/M_1$ once, namely in the second square bracket before the parentheses. This results in the following expression:

$$D[M_1/a_1 + D(1/b_1 - 1/b_3)]/(a_1/M_1)[M_1/a_1 + D(1/b_1 - 1/b_3)] \qquad \text{(B.14)}$$

Note that the terms in square brackets in the numerator and in the denominator of Eq. (B.14) cancel each other, leaving the expression $M_1(D/a_1)$. Hence, the etendue (and therefore the photosignal) for out-of-focus targets is equal to the etendue for in-focus targets. This approximation applies to cases for which the defocusing is moderate, that is where $b_3 - b_1 \ll f$.

For targets placed beyond the focal plane, the target diameter is given by

$$M_2 = (a_2/a_1)(M_1 + D) - D \qquad \text{(B.15)}$$

A similar geometrical analysis as given in the preceding shows again that the signal for out-of-focus targets is the same as for in-focus targets. This very important feature of pyrometers is key to their use in factory application.

BIBLIOGRAPHY

1. M. Bass (ed.) *Handbook of Optics*, New York: McGraw-Hill, 1995, chap. 1, p. 13.
2. M. Bass (ed.) *Handbook of Optics*, New York: McGraw-Hill, 1995, chap. 1, p. 15.
3. Hamamatsu Corporation, Tech. Inf. SD-12, July 1993, p. 11.
4. J. Sunderland US Patent No. 3,795,918 , 1974.
5. H. Rubin *Ann. Phys.*, **18**: 725 (1905).
6. A. Stein *6th Int. Congr. Appl. Lasers Electro-optics*, 1987, p. 29.
7. *The Infrared Handbook*, Washington, DC: Office Naval Res., 1978, pp. 20–27.
8. Product literature from companies: Impact Electronic GmbH, Quantum Logic Corp., and Williamson given in Table 1.
9. M. Bass (ed.) *Handbook of Optics*, New York: McGraw-Hill, 1995, chap. 13, p. 15.
10. Advanced Crystal Products, Woughburn, MA.
11. *Optical Fiber Brochure*, Oxford, UK: Oxford Electronics Ltd.
12. A. Stein US Patent No. 4,708,493 and European Patent No. EP0317653 B1..
13. G. Koska J. Reger *VDI Berichte 1379, Temperature '98*, p. 227.
14. A. T. Fiory *et al. Mater. Res. Soc. Symp. Proc.*, **303**: 139, 1993.
15. B. Nguyenphu M. Oh A. T. Fiory Temperature monitoring by ripple pyrometry in rapid thermal processing, *Mater. Res. Soc. Symp. Proc.*, **429**: 1996, pp. 291–296.
16. P. B. Coats *Metrologia*, **17**: 103–109, 1981.
17. T. P. Murray *Rev. Sci. Instr.* **38**: 791, 1967.

READING LIST

J. T. Quinn *Temperatures*, New York: Academic Press, 1983.

ALEX STEIN
Quantum Logic Corporation